

A TWO-DIMENSIONAL MODEL FOR THE HEAP BIOLEACHING OF CHALCOCITE: EFFECT OF INLET HEIGHT

Martin J. LEAHY¹, Malcolm R. DAVIDSON² and M. Phil SCHWARZ¹

¹CSIRO Minerals, PO Box 312, Clayton South, Melbourne Victoria, 3169, Australia

²Department of Chemical and Biomolecular Engineering, The University of Melbourne, Victoria, 3010, Australia

ABSTRACT

A two-dimensional (2D) model of the heap bioleaching of chalcocite and pyrite is given, which accounts for the placement of spargers inside the heap. The 3-phase finite volume computational fluid dynamics model accounts for the transport of air, liquid and heat in the heap, in addition to the reaction of chalcocite and pyrite in the solid, and attachment of bacteria to the solid phase. This work is concerned with the 2D air flow in the heap, and it is found that the heap leaches in a 2D manner around the air inlet, and in an essentially one-dimensional manner from the top of the heap. In all inlet height cases tested, a leaching front develops from the air inlet which spreads out in all directions, and moves faster below the air inlet, than directly above the inlet. As the air inlet height is increased, the leaching is more extensive at the base due to there being more room for the leaching front to spread into. However, if the inlet is positioned too high, the air flow is poor at the base of the heap, and consequently oxygen limitation becomes the most important factor. An explanation for these mechanisms is given.

NOMENCLATURE

Q	heat source term, (W/m^3)
R_k	reaction rate for reaction k , ($kg/m^3/s$)
T	temperature, ($^{\circ}C$)
\mathbf{v}	air velocity vector, (m/s)
v_L	liquid velocity, (scalar and negative) (m/s)
Greek	
α_T	cumulative copper extracted, (-)
ρ_i	density phase i , (kg/m^3)
μ_i	dynamic viscosity phase i , ($kg/m/s$)
ε_i	volume fraction phase i , (-)

INTRODUCTION

The hydrometallurgical process known as heap bioleaching can take place over a period of months to years (Bartlett, 1998), and is performed on low grade ore often including copper-sulfides and pyrite. The heaps are large piles and are leached with applied acidic solution. The heap bioleaching process involves the presence of bacteria (occurring either naturally or seeded in solution). The injection of air into the heap (sparging) is of upmost importance to keep the aerobic bacteria alive, for optimal leaching. The solution soaks into the ore and leaches the metal into a solution which is then collected and processed.

Dixon (2000) investigated the 1D heat balance in a heap with a simple reaction model, with constant and uniform liquid flow, constant reaction species and heat generation.

A number of more complex heap and column bioleaching models which also include heat balance have been developed in the last decade. These include the work of Dixon and Petersen (2003), and Ogbonna et al. (2005), who developed models incorporating copper-sulfide and sulphur oxidation, iron and sulfur oxidizing bacteria, including bacterial growth, death and transport, precipitation of jarosite, two stage leaching (for chalcocite), acidity (pH), and multiple particle sizes (Bennett et al., 2003). Various ore types and chemical and biochemical processes have been considered; in particular, chalcocite heap bioleaching (Dixon, 2000), zinc sulphide heap bioleaching (Dixon and Petersen, 2004), thermophilic column bioleaching of chalcopyrite concentrates (Petersen and Dixon, 2002), and pyrite heap bioleaching (Ritchie, 1997). However, these studies contain little analysis of the spatial profiles of the temperature, mineral extraction, bacterial concentrations and ferric and ferrous ion concentration. Furthermore, there has been little consideration of the complex reaction and associated heat balance for ore containing chalcocite and pyrite. Recently, Leahy et al. (2005a) discussed the spatial profiles of a heap bioleaching model for chalcocite and pyrite with a 1D air flow model. In Leahy et al. (2005b), a discussion of two-dimensional (2D) air flow is given, but the model is taken to be isothermal. The aim of this paper is to extend these discussions to the non-isothermal case with 2D air flow, and to investigate the interaction between oxygen, bacteria, temperature and the associated chalcocite leaching behaviour. An investigation of the effect of inlet height is given.

MODEL DESCRIPTION

Assumptions

As shown in Figure 1, the model simulates a columnar section of the heap bed associated with one air sparger pipe. The two-dimensional assumption used here would apply if the spacing between holes along the pipe was much less than the spacing between pipes.

In practice the particle size distribution can be widely varying, with regions of different permeability and porosity through the bed. In this work we assume a uniform heap. We also assume water and acid solution feeds uniformly downward under the influence of gravity, though in practice the solution flow can take tortuous flow paths, with liquid channelling and stagnant liquid regions (Bouffard and Dixon, 2001).

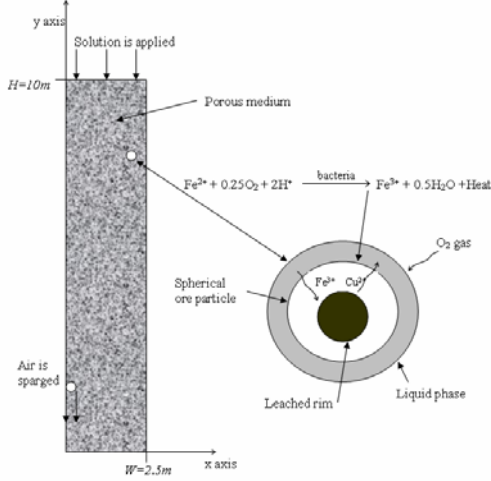
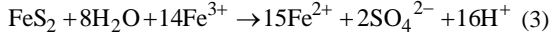
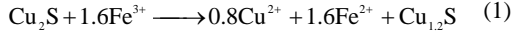


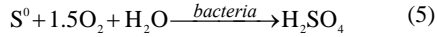
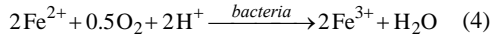
Figure 1: Schematic geometry of heap section. Air is sparged from a point source within the porous heap. Schematic shrinking core kinetics also shown.

Reactions

As shown schematically in Figure 1, ferric ions are used in intra-particle leaching of copper, to produce ferrous and copper ions in solution (reactions (1) and (2)) for the two stage leaching of chalcocite (Dixon and Petersen, 2003), and in the dissolution of pyrite (reaction (3)).



Ferrous ions are re-oxidized to ferric ions in the presence of bacteria (only *Acidithiobacillus ferrooxidans* is considered) as



Sulfur and iron oxidizing acidophilic bacteria such as *Acidithiobacillus ferrooxidans* are involved when ferrous ions are catalyzed to ferric ions (equation (4)), which increases the overall reaction rate significantly (Meruane and Vargas, 2003). Elemental sulfur produced in equation (1) may also be oxidized by *A. ferrooxidans* (Nemati et al., 1998) and *Sulfobacillus*-like bacteria as in equation (5). The optimal growth of bacteria is strongly coupled with iron, sulfur, oxygen, temperature and pH levels.

Air Flow

Air is sparged into the heap as shown in Figure 1. The air flow is described by the equation of continuity (equation (6)) and the Navier-Stokes (N-S) equations (equation (7)), with the last two terms in (7) due to buoyancy and porous media resistance (Al-Khlaifat and Arastoopour, 1997), respectively. More details are given in Leahy et al. (2004), and the 2D equations are given by

$$\nabla \cdot \mathbf{v} = 0 \quad (6)$$

$$\rho_{a,0} \frac{\partial \mathbf{v}}{\partial t} + \rho_{a,0} \nabla \cdot (\mathbf{v}\mathbf{v}) = -\nabla p + \mu_a \nabla^2 \mathbf{v} - \frac{\varepsilon_a \mu_a}{K} \mathbf{v} + \rho_{a,0} (1 - \gamma(T - T_0)) \mathbf{g} \quad (7)$$

where p (N/m²), \mathbf{v} (m/s), μ_a (kg/m/s), $\rho_{a,0}$ (kg/m³), T_0 (K), \mathbf{g} (m/s²), γ (1/K), ε_a (void m³/total m³), K (m²) are the air pressure, interstitial velocity, viscosity and density (at

atmospheric conditions), buoyancy reference temperature, gravitational vector, thermal expansion coefficient of air, porosity and permeability of the heap, respectively. For low flow rates (as in this work) and in the limit of large resistance, equation (7) represents Darcy flow. For simplicity, we revert to the use of the symbol ρ_a (kg/m³) for the constant air density instead of $\rho_{a,0}$ in the rest of this work. The superficial air flow rate at the air inlet is set to a typical value used in practice, at $q_{inlet} = 4.89 \times 10^{-3}$ (m/s), which gives interstitial air velocity at inlet of

$$v_{inlet} = q_{inlet} / \varepsilon_a = 2.44 \times 10^{-2} \text{ (m/s)}.$$

Liquid Flow

The liquid is assumed to be applied evenly to the top of the heap, and is assumed to flow vertically (as shown in Figure 1), and to have a negligible effect on the flow of air, except to cool it. We use a constant interstitial liquid velocity within the heap ($v_L = -6.75 \times 10^{-6}$ m/s). The transport equation for the j th liquid species C_j (kg/m³) at time t (seconds) is given by the advection-diffusion equation for the species in liquid: dissolved oxygen (e.g. C_L (kg/m³)), free bacteria, ferrous ions and ferric ions as

$$\frac{\partial(\varepsilon_L C_j)}{\partial t} = D_L \nabla^2 C_j - v_L \frac{\partial(\varepsilon_L C_j)}{\partial y} + S_{L,j} \quad (8)$$

where ε_L is the volume fraction of liquid, D_L is the diffusion (and dispersion) coefficient for the species in the liquid phase, and $S_{L,j}$ (kg/m³/s) is the source/sink term for the j th species. This term represents the source/sink for each species and represents attachment/detachment, bacterial growth and death, oxygen and ferrous ion consumption, and ferric ion regeneration for the respective species as outlined above. More details of the source terms, and description of attached bacteria are given in Leahy et al. (2005a).

Oxygen Balance

The scalar equation for the air oxygen concentration C_a is given by the well known advection diffusion equation in unsaturated porous media for air occupying a volume fraction ε_a

$$\frac{\partial C_a}{\partial t} = \rho_a D_a \nabla^2 C_a - \rho_a \nabla \cdot (C_a \mathbf{v}) + k_L (C_L - H_e C_a) \quad (9)$$

where D_a (m²/s) is the diffusion coefficient of oxygen in air, and the last term in (9) is the source term for the oxygen in air, representing the first order oxygen mass transfer rate between air and the liquid phase. H_e (-) is the Henry's Law coefficient, dependent on temperature as in Leahy et al. (2005).

Energy Balance

It is assumed heat transfer kinetics can be neglected, due to the low flow rates and an equilibrium heat balance model can be used (Dixon, 2000). The total heat balance is the summation of the enthalpy over the three phases (liquid, air and solid), and is given by

$$\sum_{i=a,l,s} \varepsilon_i \rho_i C_i \frac{\partial T}{\partial t} = k_B \nabla^2 T - \nabla \cdot (\varepsilon_a \rho_a C_{p,a} T \mathbf{v}) - \varepsilon_L \rho_L C_{p,L} v_L \frac{\partial T}{\partial y} + Q \quad (10)$$

where T (°C) is the temperature, $C_{p,i}$ (J/kg°C) is the specific heat, k_B is the total (of all three phases) thermal conductivity (W/m°C), Q (W/m³) is heat source term, and

a, l and s correspond to air, liquid and solid phases respectively. The heat source term is written in terms of the latent heat released or consumed during evaporation or condensation (first term in (11)), and the (second term in (11)) is the sum of heat source or sinks due to reaction equations (1)-(5) as

$$Q = -\lambda_{latent} S_w + \sum_{k=1}^5 \Delta H_k R_k \quad (11)$$

where R_i is rate of reaction i (equations (1)-(5)), ΔH_k is the heat of reaction for k^{th} reaction, S_w is the mass of water transferred during evaporation or condensation of water, λ_{latent} is the latent heat of evaporation. More detail of S_w is given in Pantelis et al. (2002), and more details of the reaction rates R_k are given in Leahy (2006). Suffice to say the shrinking core model is used for reactions (1)-(3), and Monod kinetics are used for reactions (4)-(5).

Boundary and Initial Conditions and Numerical Considerations

Initially, the heap is assumed to have a uniform population of bacteria in solution (10^{14} bacteria/m³), zero attached population, atmospheric levels of oxygen, ferrous and ferric ion concentration of 1 kg/m³, and an initial heap temperature of $T_0=25^\circ\text{C}$. At the top and bottom of the heap, the gradients for the species concentrations in the air and liquid phases at their respective exits are assumed to be zero. The ferrous and ferric ion concentration applied to the top of the heap are taken to be 1 kg/m³, whilst bacteria are not added to the top of the heap. The inlet air phase oxygen concentration is taken to be atmospheric. The boundary conditions for the temperature are constant at the air and liquid inlets with a temperature of $T_0=25^\circ\text{C}$. Parameters used in all simulations are not shown due to the extensive list, but are given by Leahy et al. (2005a), along with more details of the boundary conditions. The columnar section of bed simulated is assumed to be part of a repeating pattern associated with every air pipe, so symmetry boundary conditions are used on both the left and right hand sides in Figure 1. CFX4.4 (2001) is used to solve the coupled fluid dynamics and species and heat balance equations, together with the boundary and initial conditions specified above.

RESULTS

Inlet Height 1m

The inlet is placed at 1m from the base of the heap (as shown schematically in Figure 1). The air flow vector field is shown in Figure 2a, coloured by the log of the speed, and a scalar plot of the log of the speed is shown in Figure 2b. At the air inlet in Figure 2, the air velocity is largest (and downwards) and declines rapidly due to the resistance of the porous medium. The air flow is still significant at the right edge of the heap, despite being 2.5m from the inlet. The air moves back upwards because of the combination of the bottom of the heap (essentially a wall) and the right symmetry condition allowing no flux of air through these boundaries. Above the inlet, above a certain height, the air velocity becomes uniform over space as shown in the speed plot in Figure 2b. The speed of the air in this uniform region is also equal to the air velocity which would result if the inlet was across the whole bottom of the heap, or the overall air flow rate per unit area. This property is due to conservation of mass of air. Figure 3a-d shows a spatial plot of the temperature

distribution in the heap at various times, showing cooling near the liquid and air inlets, and high temperature throughout the majority of the heap 17.4 to 231.5 days. This behaviour is similar to the 1D results presented in Leahy et al. (2005a), where the heap heats up over the majority of the heap away from the inlets, due to the high initial bacterial concentration allowing production of heat until the conditions become too hot, as shown by the bacterial concentration distribution in Figure 4a-d.

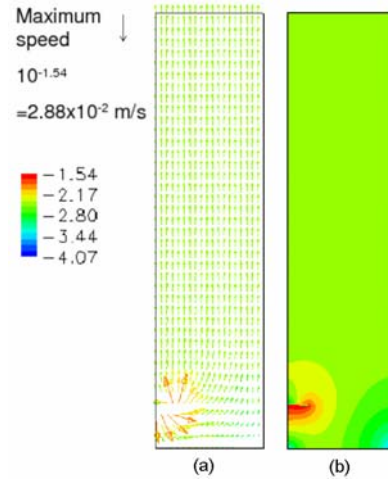


Figure 2: (a) Vector field \mathbf{v} (m/s) plot and (b) scalar plot log of speed $|\mathbf{v}|$ (m/s) at 231.5 days. 1m inlet height.

However, due to the 2D air flow, a 2D leaching front develops which moves away from the air inlet in all directions (Figures 3, 4 and 5). Figure 3 shows the temperature front moving as a semi-circular front, reaching the bottom of the heap and spreading out as a half semi circle. Figures 4 and 5 show the bacterial concentration and local copper extracted also moving as a semi-circular front, respectively. The bacterial concentration is highest near both air and liquid inlets, whilst being lowest in the overheated region.

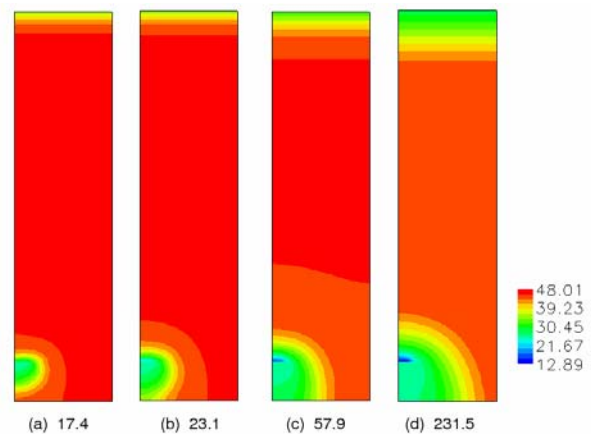


Figure 3: Temperature T ($^\circ\text{C}$) at (a) 17.4, (b) 23.1, (c) 57.9 and (d) 231.5 days. 1m inlet height.

The leaching front at the top of the heap is essentially unchanged from the 1D results in Leahy et al. (2005a), with a top-down front due to the cooling provided by the incoming cool liquid. This is not unexpected, because the air flow is essentially 1D at the top of the heap. In the

latter stages of the simulation, the temperature near the air inlet in Figure 3c,d is very low, as low as 12.9°C, which is less than the temperature boundary condition of $T_0=24.85^\circ\text{C}$. The temperature may drop below that of the boundary condition temperature only if the latent heat evaporative term at any region is greater (negative) than the heat produced (positive) there. The latent heat evaporative term is greatest (negative) where there are large gradients in the air velocity. As shown in Figure 2b, the maximum velocity is relatively large (around 2×10^{-2} m/s) at the air inlet, and the air velocity quickly reduces as it experiences resistance in the heap, thus a large gradient in the velocity exists near the inlet.

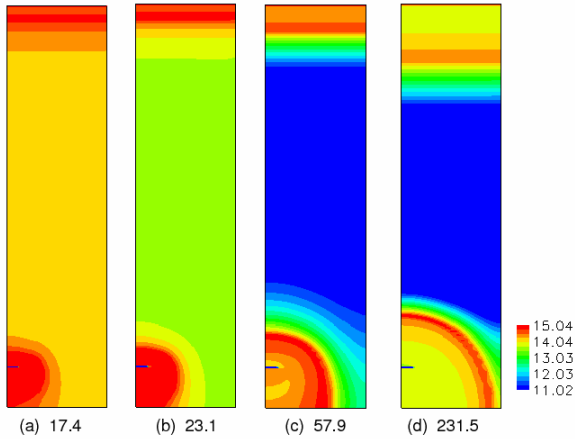


Figure 4: log of bacterial concentration per m^3 at (a) 17.4, (b) 23.1, (c) 57.9 and (d) 231.5 days. 1m inlet height.

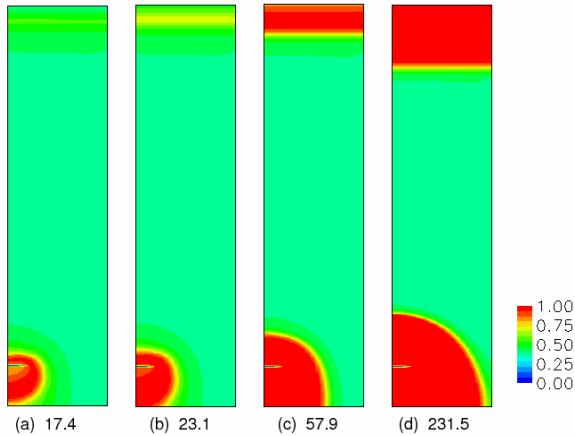


Figure 5: local copper extracted α (-) at (a) 17.4, (b) 23.1, (c) 57.9 and (d) 231.5 days. 1m inlet height.

Inlet Height 2.5m

We now position the inlet 2.5m from the base of the heap, and a similar flow field to that of the 1m case is achieved (not shown), but is shifted up to 2.5m from the base. The plot of the local copper extracted in Figure 6a-d shows that the leaching front below the inlet moves away from the air inlet faster than directly above or sideways from the air inlet. Eventually the front runs out of room, as shown in Figure 6d. Due to the extensive leaching below the inlet, the cumulative copper extracted for 2.5m inlet is $\alpha_T=65.3\%$, compared to $\alpha_T=58\%$ for the 1m inlet; this is due to there being more room for leaching below the air inlet. It may be that an even higher inlet position (next

section) will allow more room for fast leaching below the air inlet. The leaching front moves faster downwards, more rapidly than sideways or upwards from the air inlet because the gas phase heat advection (which is cooling) does not encounter heating from the liquid advection of heat downwards.

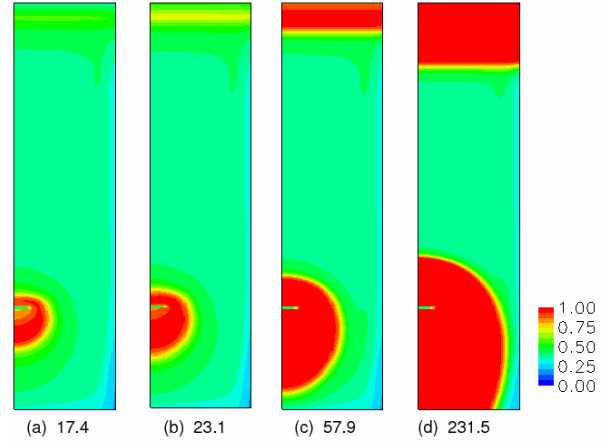


Figure 6: local copper extracted α (-) at (a) 17.4, (b) 23.1, (c) 57.9 and (d) 231.5 days. 2.5m inlet height.

Inlet Height 5m

We now position the inlet 5m from the base of the heap, half way between the bottom to the top of the heap unit. Figure 7a-b gives the vector field and plot of the log of the speed for this case. In this case the inlet is so far from the bottom of the heap (5m) that extremely small air velocities are experienced below the inlet over a large region, approximately the bottom quarter of the heap. Indeed, air velocities as low as $10^{-5.9} \text{ms}^{-1} = 1.26 \times 10^{-6} \text{ms}^{-1}$ are observed in the bottom left and right hand corners of the unit heap.

Figures 8, 9, 10 and 11 show spatial distribution plots at different times (for the 5m inlet) of the normalized oxygen concentration in liquid, temperature, total bacterial concentration and local copper extracted, respectively. It is now appropriate to show the oxygen concentration plot, because parts of the heap are limited by oxygen at certain stages.

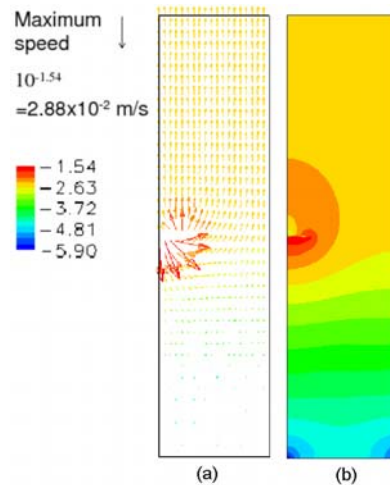


Figure 7: (a) Vector field \mathbf{v} (m/s) plot and (b) scalar plot log of speed $|\mathbf{v}|$ (m/s) at 231.5 days. 5m inlet height.

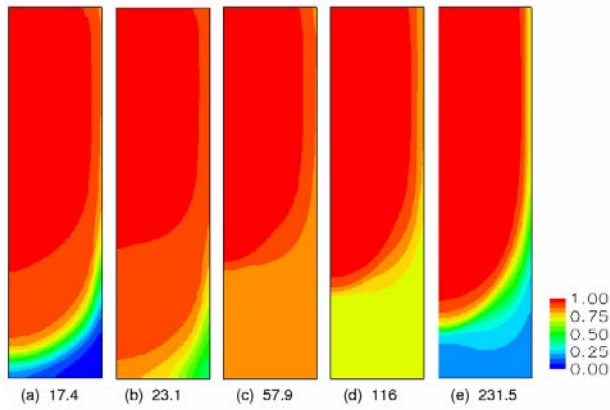


Figure 8: Oxygen concentration in liquid normalized (-) at (a) 17.4, (b) 23.1, (c) 57.9 and (d) 116 and (e) 231.5 days. 5m inlet height.

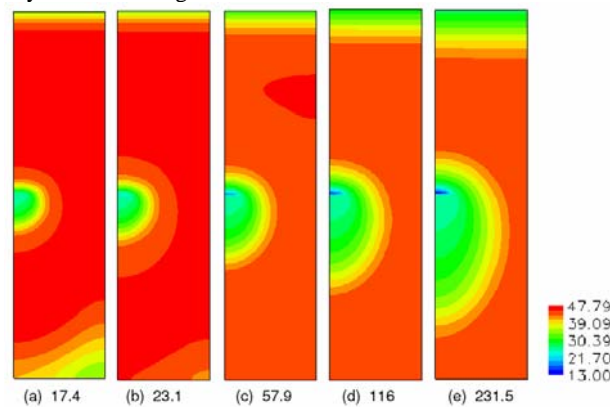


Figure 9: Temperature (°C) at (a) 17.4, (b) 23.1, (c) 57.9 and (d) 116 and (e) 231.5 days. 5m inlet height.

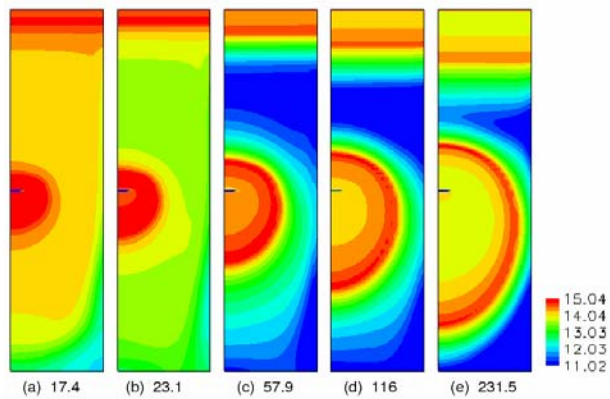


Figure 10: log of bacterial concentration per m^3 at (a) 17.4, (b) 23.1, (c) 57.9 and (d) 116 and (e) 231.5 days. 5m inlet height.

Away from the base, no oxygen supply limitation occurs (due to high air flow) and leaching (Figure 11) in the shape of a semi circle develops (as previously with 1m and 2.5m inlet), and the usual top-down leaching (from the top) occurs. As discussed in the previous sections, these leaching fronts develop due to overheating and the cooling provided by the respective inlets. However, the dynamics of the variables in this simulation are more complex, with limitation of oxygen occurring (at the beginning) in the lower parts of the bed, with little copper extraction in that region for the rest of the time steps shown. To explain this more clearly, we draw attention to

the early stages in these Figures 8-11, looking at the first two time steps shown at 17.4 and 23.1 days. At these times it can be observed in Figure 8a and b, that the oxygen concentration is very low and relatively low, respectively, at the bottom right hand corner, the furthest point from the inlet at the base of the heap. Such low oxygen concentrations would develop early (before the time steps shown), because initially there are high bacterial concentrations throughout the whole heap (due to the initial condition specified): combined with the low air flow, low oxygen concentration occurs. This low oxygen concentration (early) leads to a low bacterial concentration in this region, (see Figure 10a,b). It is during the first two time steps shown at 17.4 and 23.1 days, that the low oxygen concentration in this region (and resultant low bacterial concentration) prevents leaching occurring before the heap has become too hot; elsewhere in the heap (during these early times) where there is no oxygen shortage, the heap leaches quickly before it becomes too hot, and this accounts for a significant amount of leaching, up to 50% locally (Figure 11a). This region does not recover since overheating occurs, with the bacterial concentration remaining low.

At the middle/latter stages of Figure 9 at 57.9, 116 and 231.5 days, it can be observed that the heap heats up everywhere (including the low deoxygenated bottom right hand corner), except near the inlets, and the only significant leaching that occurs is due to the leaching fronts at the cool air and liquid inlets. In the middle/latter time period, the leaching spreading in all directions from the air inlet can be considered to be the same as described for the 2.5m inlet placement. However in this case (5m inlet) the front below the inlet does not run out of room for leaching, which occurs in the 2.5m case, when the leaching front reaches the base of the heap. Therefore, the benefits of higher inlet and improved leaching, need to be weighed up against the oxygen supply limitation which occurs at the base. Overall the copper extraction is very similar to that of the 2.5m inlet, with $\alpha_T=64.7\%$ for 5m case, compared to $\alpha_T=65.3\%$ for the 2.5m case, and $\alpha_T=58\%$ for the 1m case. The extra leaching around the leaching front near the air inlet (higher inlet corresponds to more leaching below the inlet) is countered by the lower leaching at the base due to the early oxygen supply limitation. It can therefore be concluded that the optimum height of the sparger is between 2.5m and 5m, to gain the extra leaching due to the greater downwards speed of the leaching front around the inlet, but avoiding early oxygen supply limitation, that lasts throughout the simulation.

CONCLUSION

A 2D air flow model of heap bioleaching was considered, where the air inlet was placed inside the heap at heights of 1m, 2.5m and 5m. At each inlet height, the 2D air vector field affects the oxygen and temperature distribution and causes the reaction variables to have 2D spatial dependence, due to the coupling of air flow and temperature, and thus other variables. A leaching front from the air inlet spreads out in all directions from the air inlet. The front moves faster immediately below the inlet than above the inlet, which is because there is less heating below front than above, and thus more cooling for the leaching front below the inlet; this is due to the direction

of the liquid advection being downwards. As the inlet height was increased, the copper extraction below the air inlet improved due to the leaching front having more room to move downwards away from the air inlet. However, when the air inlet was high (5m), the oxygen concentration at the base reduced due to a lack of air advection, causing oxygen supply limitation (initially) lasting through the simulation results. The oxygen supply limitation at the base was significant enough to negate the improved leaching around the lower leaching front (around the inlet) due to the high inlet position. Further work should investigate the effect of reduction of the air flow rate to reduce overheating, and the interaction of mesophiles with moderate thermophiles.

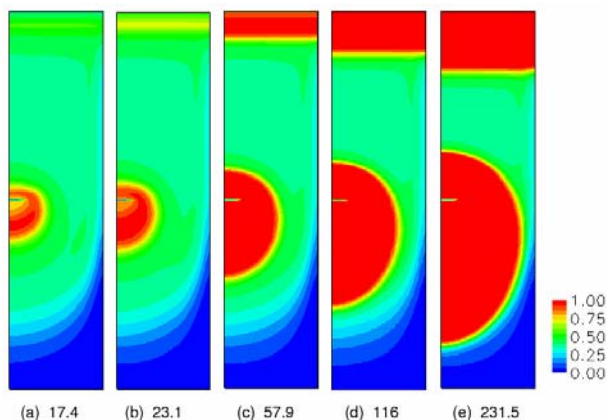


Figure 11: local copper extracted α (-) at (a) 17.4, (b) 23.1, (c) 57.9 and (d) 116 and (e) 231.5 days. 5m inlet height.

ACKNOWLEDGMENTS:

The help of Peter Witt with CFX, Helen Watling with experimental aspects, Jakub Bujalski with modelling aspects, as well as funding from an Australian Postgraduate Award and a CSIRO top-up scholarship (for M.J. Leahy) was greatly appreciated.

REFERENCES

AEA Technology, CFX-4.4: Solver, AEA Technology, Harwell Laboratory, Oxfordshire, UK, (2001).

AL-KHLAIFAT, A. and ARASTOPOUR, H. (1997), "Simulation of two-phase flow through low-permeability porous media", AEA technology international user conference '97.

BARTLETT, R., (1998), "Solution Mining: Leaching and fluid recovery of materials, 2nd edition", The Netherlands : Gordon and Breach Science Publishers.

BENNETT, C.R., CROSS, M., CROFT, T.N., UHRIE, J.L., GREEN, C.R., and GEBHARDT, J.E., (2003), "A comprehensive copper stockpile leach model: background and model formulation", in *Hydrometallurgy 2003, Volume 1: Leaching and Solution Purification*, 315-328, (TMS).

BOUFFARD, S.C. and DIXON, D. (2001), "Investigative study into the hydrodynamics heap leaching processes", *Met. Mat. Trans.*, **32B**, 899-909.

DIXON D.G. (2000), "Analysis of heat conservation during copper sulphide heap leaching", *Hydrometallurgy*, **58**, 27-41.

DIXON D.G. and PETERSEN, J. (2003), "Comprehensive modelling study of chalcocite column and heap bioleaching", in *Copper 2003-Cobre 2003 Volume VI - Hydrometallurgy of Copper (Book 2)*, pp 493-515.

DIXON D.G. and PETERSEN, J. (2004), "Modeling the dynamics of heap bioleaching for process improvement and innovation", in *Hydrosulfides 2004, Proceedings of the International Colloquium on Hydrometallurgical Processing of Copper Sulfides*, pp 13-45.

LEAHY, M.J., DAVIDSON, M.R. and SCHWARZ, M.P., (2005a), "A model for heap bioleaching of chalcocite with heat balance: bacterial temperature dependence", *Minerals Engineering*, **18**, (13-14), 1239-1252.

LEAHY, M.J., DAVIDSON, M.R. and SCHWARZ, M.P., (2005b), "A two-dimensional CFD model for heap bioleaching of chalcocite", *ANZIAM J.*, **46**(E), C439-C457.

LEAHY, M.J., (2006), PhD thesis, "Temperature and Air Flow Effects in the Modelling of Bacteria in Heap Bioleaching of Chalcocite", The University of Melbourne, Australia.

MERUANE, G and VARGAS, T. (2003), "Bacterial oxidation of ferrous iron by *Acidithiobacillus ferrooxidans* in the pH range 2.5-7.0", *Hydrometallurgy*, **71**, 149-158.

NEMATI, M., HARRISON, S., HANSFORD, G. and WEBB, C., (1998), "Biological oxidation of ferrous sulfate by *Thiobacillus ferrooxidans*: a review on the kinetic aspects", *Biochemical Engineering Journal*, **1**, 171-190.

OGBONNA, N., DIXON D.G. and PETERSEN, J. (2005), "HeapSim - unravelling the mathematics of heap bioleaching", in *Computational Analysis in Hydrometallurgy 35th Annual Hydrometallurgy Meeting*, pp 225-240, MET SOC.

PANTELIS, G., RITCHIE, A., and STEPANYANTS, Y., (2002), "A conceptual model for the description of oxidation and transport process in sulphidic waste rock dumps", *Appl. Math. Mod.*, **26** (2), 751-770.

PETERSEN, J. and DIXON D.G. (2002), "The dynamics of chalcocite heap bioleaching", in *Hydrometallurgy 2003, Volume 1: Leaching and Solution Purification*, pp 351-364, (TMS).

RITCHIE, A. (1997), "Optimization of biooxidation heaps", in *Biomining: Theory, microbes and industrial processes*, Ed: D.E. Rawlings, Springer.